High-yield bamboo-shaped carbon nanotubes from cresol for electrochemical application†

Ruitao Lv,[a] Lin Zou,[a] Xuchun Gui,[b] Feiyu Kang,*[a] Yanqiu Zhu,[c] Hongwei Zhu,[d] Jinquan Wei,[b] Jialin Gu,[a] Kunlin Wang[b] and Dehai Wu[b]

Received (in Cambridge, UK) 8th January 2008, Accepted 28th January 2008
First published as an Advance Article on the web 20th February 2008
DOI: 10.1039/b800233a

High-yield bamboo-shaped carbon nanotubes (BCNTs) have been produced by using cresol as the precursor, for the first time and there are almost no straight CNTs or amorphous carbon found in the product: the role of cresol in promoting the growth of BCNTs is discussed; improved cycle stability and electric conductivity of the BCNTs as an anode additive in a lithium ion battery are achieved.

As an important member of the carbon nanotube family, bamboo-shaped carbon nanotubes (BCNTs), with separated hollow compartments, have been widely investigated to explore their unique structure-associated properties.[1–4] BCNTs possess a high percentage of edge–plane sites along the surface, and are thus expected to exhibit improved electrochemical characteristics compared with their straight CNT counterparts with smooth, more basal plane-like regions.[5,6] In particular, BCNTs also showed a faster electron transfer rate and a greater number of electroactive sites than single-walled carbon nanotubes in the biosensing of guanine and adenine.[7]

Several techniques have been used to prepare BCNTs, such as plasma enhanced chemical vapor deposition (PECVD),[8,9] radio frequency magnetron sputtering,[10] electric arc discharge,[11] powder pyrolysis,[3,7,12,13] substrate growth,[1,2,14–16] ball milling[17] and the exploding method,[18] and significant progress has been made recently. However, most of these approaches have apparent disadvantages, for example, expensive equipment,[8–10] low yield,[11] poor growth control[3,18] and often they are not suitable for continuous production.[1,2,14–16] The manufacturing of high purity materials in large quantity remains a real technical challenge. In this context, to eliminate the co-existence of 'normal' straight multi-walled CNTs (MWNTs) and amorphous carbon in a controllable and reproducible manner, whilst achieving all BCNTs, will be of technical importance.[3,4] Existing reports use methane,[1,8] graphite rods,[10,11] ruthenium(III) acetylacetonate,[3,19] iron(II) phthalocyanine,[13] *etc.* as precursors and, to the best of our knowledge, cresol has not been applied as a precursor. We will report that cresol is not a simple replacement chemical for the growth of CNTs, but a novel, efficient and on-purpose precursor for high-yield BCNT production.

The experimental setup and procedure are similar to that described previously for the synthesis of FeNi-filled CNTs,[20] but cresol rather than dichlorobenzene was used as the carbon source. In a typical process, ferrocene was dissolved in 10 ml cresol to form a solution with a concentration of 0.06 g ml^{-1} which was fed into the CVD reaction tube by a syringe pump at a constant rate of 0.12 ml min^{-1}, for 30 min. A mixture of Ar and H_2 at flow rates of 2000 sccm and 300 sccm, respectively was used as the carriage gas. A quartz plate was placed in the middle of reaction tube (860 °C) for sample collection, for later characterization and evaluation by using a scanning electron microscope (SEM, JEOL JSM-6460LV) and a transmission electron microscope (TEM, JEOL-2010).

Electrochemical testing samples were prepared by mixing BCNTs (5 wt%), natural flake graphite (85 wt.%, Chenzhou, China) and polyvinylidene fluoride (PVDF 10 wt.%). The mixture was dissolved in *N*-methylpyrrolidone (NMP) and casted on a copper foil which was dried at 80 °C for 8 h and then dried in vacuum at 120 °C for 12 h. Lithium foil was used as the counter electrode and 1 M $LiPF_6$ dissolved in a mixture of ethyl methyl carbonate (EMC) and dimethyl carbonate (DMC) (1 : 1 in volume) as the electrolyte. The working and the counter electrodes were separated with a Celgard 2400 separator. The cell was galvanostatically cycled between 0 and 2.00 V *vs.* Li/Li^+ at 0.2 °C.

SEM observations show that the products are mainly entangled CNTs with lengths >4 μm (Fig. S1(a)†), with a pronounced bamboo-like appearance (Fig. S1(b)†). TEM examinations have confirmed that nearly all of the CNTs are bamboo-shaped, with no straight CNTs or amorphous carbon 'impurities' (Fig. S2a and S2b† and Fig. 1(a)). Fig. 1(a) also exhibits the existence of some Fe catalyst particles (arrowed). The weight percentage of Fe particles in BCNTs is ~17 wt%, calculated based on thermogravimetric analysis (Fig. S3†). Considering the density of iron is 4 times of that of carbon,[20] the volume fraction of Fe particles in BCNTs should be less than 5%. This shows the high-purity nature of as-prepared BCNTs. High-resolution TEM (HRTEM) study has showed that the walls of BCNTs are composed of intense bending and curling defects and clearly visible individual compartments.

[a] *Laboratory of Advanced Materials, Department of Materials Science and Engineering, Tsinghua University, Beijing 100084, China. E-mail: fykang@tsinghua.edu.cn; Fax: +86 10-62792911*
[b] *Department of Mechanical Engineering and Key Laboratory for Advanced Manufacturing by Materials Processing Technology of Ministry of Education, Tsinghua University, Beijing 100084, China*
[c] *Advanced Materials, School of Mechanical, Materials and Manufacturing Engineering, The University of Nottingham, University Park, Nottingham, UK NG7 2RD*
[d] *Department of Mechanical Engineering, University of Delaware, Newark, DE 19716, USA*

† Electronic supplementary information (ESI) available: The SEM, TEM images and TGA curve of the samples. See DOI: 10.1039/b800233a

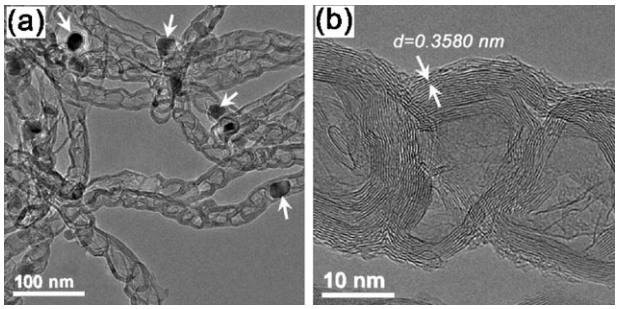

Fig. 1 Morphology of BCNTs (a) low-magnification TEM image, where the arrows show the positions of Fe catalyst particles (b) HRTEM image.

The interlayer space is ~0.3580 nm (see Fig. 1(b)), which is larger than that of planar graphite (~0.3350 nm), and that of straight CNTs (~0.3400 nm). This can be attributed to a combination of tubule curvature and van der Waals force interactions between successive graphitic layers.[21]

In order to verify the role of cresol in the BCNTs growth, controlled experiments were carried out by using xylene as a carbon precursor, which resulted in no BCNTs but well-aligned straight CNTs (see Fig. S4†). It was obvious that due to the involvement of the [OH] group in cresol, the pyrolysis routes of the two precursors would be different. It is likely that xylene and cresol may contain dominant species at some stage *via* the following process:[22]

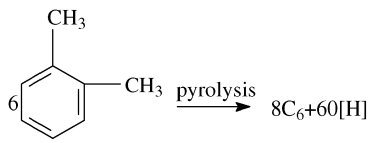

(1)

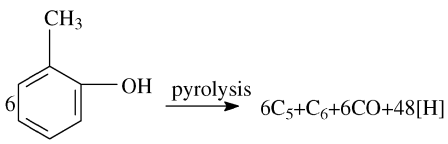

(2)

Here C_5 and C_6 denote the 5- and 6-carbon rings, respectively; and [H] denotes the active hydrogen atom. As shown in eqn (1) the 6-carbon species, presumably arranged into hexagon rings, would favour the growth of straight CNT walls as they are constructed by 6-carbon rings. When 5-carbon rings (pentagons) are introduced into the hexagon networks, as shown in eqn (2), graphitic stacking in CNTs will become irregular, (*e.g.* bamboo-shaped CNTs, heterojunctions, *etc.*).[23,24] Typically, in contrast to heptagons, 5-carbon pentagon rings are capable of constructing positive curvatures, thus promoting the formation of cone-like shapes in CNTs,[25] which is in agreement with the TEM results (Fig. 1). In this context, the pyrolysis of cresol might have well played a role in supplying a sufficient amount of pentagons, thus leading to the growth of BCNTs. The strain introduced by the pentagons renders the BCNTs defective and thus chemically reactive.[26] Fig. 2 is a Raman spectrum of the as-prepared BCNTs. The intensity of the D-band is higher than that of the G-band, indicating the extensive defects contained in the BCNT structures.

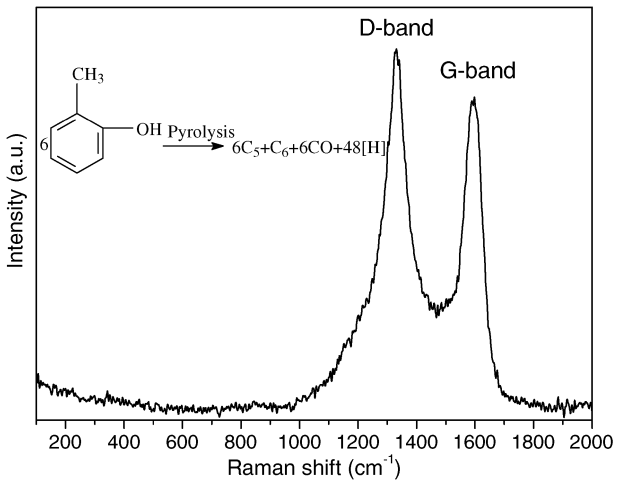

Fig. 2 Raman spectrum (633 nm excitation) of the BCNT sample.

The electrochemical performance of the BCNTs was evaluated against the commercial carbon black (CB) and straight MWNTs, as an anode additive, and the results of the cycle performance are shown in Fig. 3(a). The capacity of CB and

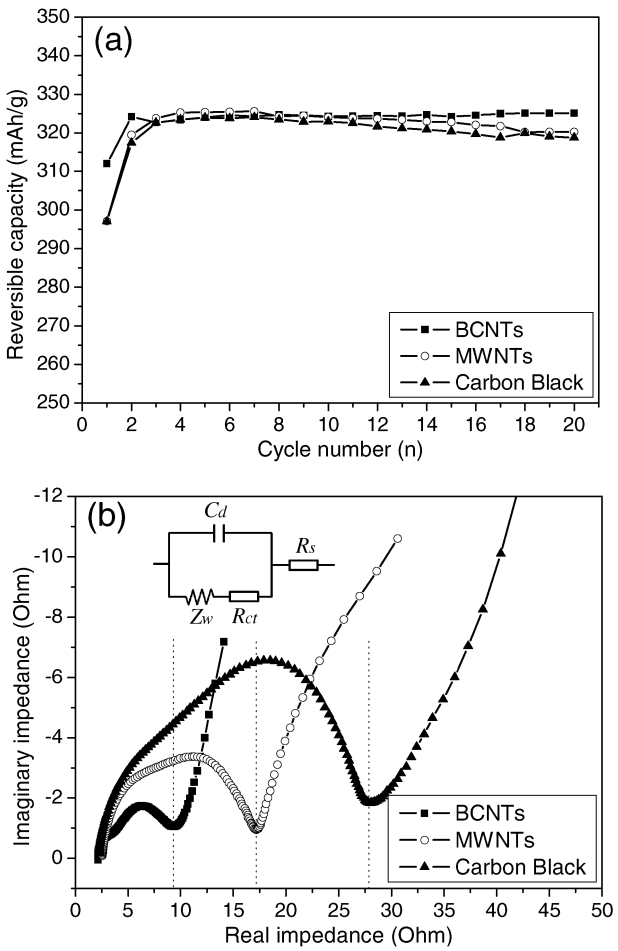

Fig. 3 Electrochemical characteristics of samples (a) cycle performances and (b) electrochemical impedance spectra of 5 wt% BCNTs, 5 wt% straight multi-walled CNTs (MWNTs) and 5 wt% carbon black in graphite anode materials.

MWNT anodes begin to decrease after 9 cycles; whilst the BCNT anode remains stable after 20 cycles. Fig. 3(b) exhibits the electrochemical impedance spectra (EIS) of the BCNT, MWNT and CB samples. They both show combinations of depressed semicircles at high- and mid-frequencies and straight line features at low-frequencies. Interpretation of the EIS was based on the equivalent circuit shown in the inset of Fig. 3(b), where C_d, Z_w, R_{ct} and R_s denote the capacitance of the double layer, Warburg impedance, charge-transfer resistance and solution resistance, respectively.

The high-frequency semicircle in the EIS is attributed to the solid electrolyte interface (SEI) film and contact resistance,[27] and the mid-frequency semicircle to the R_{ct} on the electrode/electrolyte interface. The point of the semicircle decreasing is believed to be the total electrical resistance of the electrode materials, electrolyte resistance and electric leads.[28,29] Thus, based on Fig. 3(b), the total electric resistance of the BCNTs sample is 9.3 Ω, only $\sim\frac{1}{3}$ of the CB sample's (28.0 Ω) and $\sim\frac{1}{2}$ of the MWNT sample's (17.1 Ω). This reduced resistance could lead to a much improved efficiency in battery assemblies. We believe that such a significant decrease in resistance may arise from two main factors: higher electron transfer kinetics of the BCNTs compared to that of CB and MWNTs due to the better wetability, more edge–plane-like sites and oxygen functional groups,[3] and the easy formation of three-dimensional electrical conduction networks, which is similar to the effect of general CNTs reported in our previous work on cathode additives in lithium ion batteries.[30]

In summary, we report that high-yield and high purity BCNTs have been generated *via* pyrolosis of cresol. We attribute the easy formation of 5-carbon rings during cresol pyrolysis as having a key role in the BCNT growth. As an anode additive in lithium ion batteries, BCNTs show much improved cycle stabilities and higher electric conductivity than the commercial CB. Considering the simplicity and high-efficiency of this process, we believe that cresol-generated BCNTs are excellent electrode additives for applications in lithium ion batteries.

The authors are grateful to the financial support from National Natural Science Foundation of China (Grant No. 50632040). We also appreciate the kindly help from Mr. Lin Gan with the HRTEM observation.

Notes and references

1 N. Q. Zhao, C. N. He, J. Ding, T. C. Zou, Z. J. Qiao, C. S. Shi, X. W. Du, J. J. Li and Y. D. Li, *J. Alloys Compd.*, 2007, **428**, 79–83.
2 M. Lin, J. P. Y. Tan, C. Boothroyd, K. P. Loh, E. S. Tok and Y. L. Foo, *Nano Lett.*, 2007, **7**, 2234–2238.
3 S. Shanmugam and A. Gedanken, *Electrochem. Commun.*, 2006, **8**, 1099–1105.
4 J. S. Wu, B. El Hamaoui, J. X. Li, L. J. Zhi, U. Kolb and K. Mullen, *Small*, 2005, **1**, 210–212.
5 C. E. Banks, T. J. Davies, G. G. Wildgoose and R. G. Compton, *Chem. Commun.*, 2005, 829–841.
6 R. R. Moore, C. E. Banks and R. G. Compton, *Anal. Chem.*, 2004, **76**, 2677–2682.
7 L. Y. Heng, A. Chou, J. Yu, Y. Chen and J. J. Gooding, *Electrochem. Commun.*, 2005, **7**, 1457–1462.
8 H. Cui, O. Zhou and B. R. Stoner, *J. Appl. Phys.*, 2000, **88**, 6072–6074.
9 Y. Zhou, N. Xiao, Y. F. Sun, T. J. Sun, Z. B. Zhao and J. S. Qiu, *New Carbon Mater.*, 2006, **21**, 365–368.
10 K. Y. Lee, T. Ikuno, K. Tsuji, S. Ohkura, S. Honda, M. Katayama, K. Oura and T. Hirao, *J. Vac. Sci. Technol., B*, 2003, **21**, 1437–1441.
11 Y. Saito, *Carbon*, 1995, **33**, 979–988.
12 T. Katayama, H. Araki and K. Yoshino, *J. Appl. Phys.*, 2002, **91**, 6675–6678.
13 X. B. Wang, W. P. Hu, Y. Q. Liu, C. F. Long, Y. Xu, S. Q. Zhou, D. B. Zhu and L. M. Dai, *Carbon*, 2001, **39**, 1533–1536.
14 L. J. Wang, L. L. Xie, Y. L. Li, H. Yuan, Q. H. Li and Q. Z. Li, *Acta Chim. Sin.*, 2007, **65**, 913–916.
15 J. W. Jang, C. E. Lee, S. C. Lyu, T. J. Lee and C. J. Lee, *Appl. Phys. Lett.*, 2004, **84**, 2877–2879.
16 C. J. Lee and J. Park, *Appl. Phys. Lett.*, 2000, **77**, 3397–3399.
17 Y. Chen, M. J. Conway and J. D. Fitz Gerald, *Appl. Phys. A: Mater. Sci. Process.*, 2003, **76**, 633–636.
18 Y. Lu, Z. P. Zhu, D. S. Su, D. Wang, Z. Y. Liu and R. Schlogl, *Carbon*, 2004, **42**, 3199–3207.
19 S. Shanmugam and A. Gedanken, *J. Phys. Chem. B*, 2006, **110**, 2037–2044.
20 R. T. Lv, A. Y. Cao, F. Y. Kang, W. X. Wang, J. Q. Wei, J. L. Gu, K. L. Wang and D. H. Wu, *J. Phys. Chem. C*, 2007, **111**, 11475–11479.
21 M. Terrones, T. Hayashi, K. Nishimura, M. Endo, H. Terrones, W. Hsu, N. Grobert, Y. Zhu, H. W. Kroto and D. R. M. Walton, *Tanso*, 2000, **195**, 424–433.
22 H. M. Cheng, *Carbon nanotubes—Synthesis, Microstructure, Properties and Applications*, Chemical Industry Press, Beijing, 2002.
23 B. I. Dunlap, *Phys. Rev. B: Condens. Matter Mater. Phys.*, 1992, **46**, 1933–1936.
24 L. Chico, V. H. Crespi, L. X. Benedict, S. G. Louie and M. L. Cohen, *Phys. Rev. Lett.*, 1996, **76**, 971–974.
25 M. Endo, K. Takeuchi, K. Kobori, K. Takahashi, H. W. Kroto and A. Sarkar, *Carbon*, 1995, **33**, 873–881.
26 T. W. Ebbesen, P. M. Ajayan, H. Hiura and K. Tanigaki, *Nature*, 1994, **367**, 519–519.
27 K. Fukuda, K. Kikuya, K. Isono and M. Yoshio, *J. Power Sources*, 1997, **69**, 165–168.
28 C. Y. Lee, H. M. Tsai, H. J. Chuang, S. Y. Li, P. Lin and T. Y. Tseng, *J. Electrochem. Soc.*, 2005, **152**, A716–a720.
29 Y. K. Zhou, B. L. He, W. J. Zhou and H. L. Li, *J. Electrochem. Soc.*, 2004, **151**, A1052–a1057.
30 X. L. Li, F. Y. Kang and W. C. Shen, *Carbon*, 2006, **44**, 1334–1336.

